



Studying Static Derivatives of an Inland Bulk Carrier in Open and Restricted Waters using OpenFOAM

Md. Mashiur Rahaman^{1,*}, Hafizul Islam², N.M. Golam Zakaria³, M. Ziauddin Alamgir⁴

ARTICLE INFO

Article history:

Received 17 Feb 2022;
in revised from 29 July 2022;
accepted 31 July 2022.

Keywords:

Spot Market, Demand, Container
Freight Rates (CFRs).

© SEECMAR | All rights reserved

ABSTRACT

The paper studies the maneuvering capabilities of an inland bulk carrier designed to be operated in the waterways of Bangladesh. Following the Planar Motion Mechanism (PMM) test, static drift simulations have been performed, for varying drift angles, both in open and restricted waters, to determine the linear hydrodynamic derivatives. All simulations have been performed using the open source CFD toolkit, OpenFOAM. The vessel's maneuvering capability in open and restricted water has been discussed based on the values of the derivatives. The paper concludes that although the vessel encounters substantially larger forces and moments in restricted water, channel restrictions minorly affect the static derivatives of the vessel.

1. Introduction.

Although roughly 90% of global goods are transported through shipping, almost all the goods that cross the oceans through ships end up being transported in trucks through the lands, ignoring the vast inland waterways in Europe and Asia. Like ocean-going ships, inland vessels are also relatively economical and environmentally friendly. Bangladesh, being a riverine country also relies heavily on its rivers for the transportation of goods.

Although, historically, emphasis has been limited on safety, economy, and efficiency; with an improving economy, the country has started paying attention to such aspects following global trends. As part of the effort, this paper studies the maneuvering

capabilities of a commonly used inland class vessel for carrying bulk goods.

According to International Maritime Organization (IMO) adopted Standards for ship maneuverability, a ship's safety heavily relies on its path-keeping and path-changing abilities. Thus, investigation of maneuvering derivatives during the design phase of the vessel is essential to ensure the construction of a safe and reliable vessel. Although early maneuvering studies mostly relied on experimental studies, such studies are expensive and time-consuming. Thus, with the development of Computational Fluid Dynamics (CFD) tools, more and more researchers have shifted focus to numerical studies. Planar Motion Mechanism (PMM) simulations were first widely discussed in the SIMMAN 2008 workshop (SIMMAN, 2008), where benchmark Experimental Fluid Dynamics (EFD) data was made available and compared with available CFD results. In the workshop, PMM simulation results were presented for KCS (Somonsen and Stern, 2008), KVLCC2 (Broglia et al., 2008; Cura-Hochbaum et al., 2008), and DTMB-5414 (Gullmineau et al., 2008; Miller, 2008) hull models using different CFD solvers. Following the 2008 workshop, more EFD and CFD data were made available for the SIMMAN 2014 workshop (SIMMAN 2014). Eventually, more researchers started taking interested in the topic, and more detailed CFD studies were made available like the work of Simonsel et al. (2012), Lee and Kim (2015), Shen et al. (2015),

¹Department of Naval Architecture and Marine Engineering, Bangladesh University of Engineering and Technology, Dhaka-1000, Bangladesh, E-mail: mashiurrahaman@name.buet.ac.bd.

²CENTEC, Instituto Superior Tecnico, University of Lisbon, 1049-001 Lisbon, Portugal, E-mail: hafiz2612@gmail.com.

³Department of Naval Architecture and Marine Engineering, Bangladesh University of Engineering and Technology, Dhaka-1000, Bangladesh, E-mail: gzakaria@name.buet.ac.bd.

⁴Faculty of Engineering and Technology, Bangabandhu Sheikh Mujibur Rahman Maritime University, Bangladesh, E-mail: dean.fet@bsmrmu.edu.bd

*Corresponding author: Md. Mashiur Rahaman, E-mail Address: mashiur-rahaman@name.buet.ac.bd

Kim et al. (2015), Hajivand and Mousavizadegan (2015a, b), Yao et al. (2016), Islam et al. (2017), Islam and Guedes Soares (2018a, b). However, as can be noticed, most of the studies focus on ocean-going vessels and maneuvering studies for inland vessels remain very limited (Liu et al., 2015; Liu, 2017). Furthermore, the influence of channel restrictions on maneuvering derivatives is rarely discussed. .

2. Method.

The maneuvering capabilities of an inland bulk carrier have been studied by performing PMM simulations. The OpenFOAM version 2006 has been studied for the study. The open water static drift simulations were performed with a heave and pitch free motion. However, for the restricted water simulations, heave and pitch motions have been kept restricted. lib-sixDoFRigidBodyMotion library was used for the open water static drift simulations. Simulations were performed at a high Reynolds number with turbulent flows. Details on the solver, ship model, simulation setup, and resources are given in the following subsections.

2.1. The solver.

OpenFOAM is an open-source library that numerically solves a wide range of problems in fluid dynamics from laminar to turbulent flows, with single and multi-phases. The solver has been elaborately described by Jasak (2009). The governing equations for the solver are the Navier-Stokes or momentum equation (1) and the continuity equation (2). In vector form, the Navier-Stokes and continuity equation are given by:

$$\rho \left(\frac{\partial v}{\partial t} + v \cdot \nabla v \right) = -\nabla p + \mu \nabla^2 v + \rho g \quad (1)$$

$$\nabla \cdot v = 0 \quad (2)$$

Here, v is the velocity, p is the pressure, μ is the dynamic viscosity, g is the acceleration due to gravity and ∇^2 is the Laplace operator.

The volume of fluid (VOF) method is used to model the fluid as one continuum of mixed properties. This method determines the fraction of each fluid that exists in each cell, thus tracking the free surface elevation. The volume fraction is obtained by equation (3):

$$\frac{\partial \alpha}{\partial t} + \nabla \cdot (\alpha v) = 0 \quad (3)$$

where v is the velocity field, and α is the volume fraction of water in the cell, varying from 0 to 1, with 0 representing a cell full of air and 1 representing a cell full of water.

The Finite Volume Method (FVM) is used to discretize the governing equations. Pressure-velocity coupling is obtained through the PIMPLE algorithm. OpenFOAM incorporates several turbulence models, and for the present paper, the two-equation SST $k-\omega$ model was used. Rough wall function has been used to account for the frictional resistance.

2.2. Ship model.

The studied vessel is an inland bulk carrier that is in operation in the inland waterways of Bangladesh. It is a standard 82m bulk carrier with a blunt bow and twin propellers. The vessel is designed to be 3000DWT and has a service speed of 10 knots. The design has been approved by The China Plan Approval Center, RINA. Table 1 provides the specifications of the hull model and Figure 1 shows its side view. All the simulations have been performed on a model scale.

2.3. Mesh.

For the open water simulation mesh domain, general ITTC guidelines have been used, with one and a half ship length in front of the bow, two and a half ship lengths behind the stern, one ship length at each side, one ship length for depth, and half ship length above the free water surface.

For the restricted water simulations, a class III channel was considered following the definition by Bangladesh Inland Water Transport Authority. The class III routes are feeder routes with regional importance. Such routes generally have a minimum vertical clearance of 7.62m and a horizontal clearance of 30.48m. As such, since the simulations have been performed for a 1:10 scale model, the restricted channel has been created using a draft to depth ratio of 2 (8.7m) and width of 3.8m on each side (assuming a two-way channel).

OpenFOAM mesh generation tools have been used for mesh generation. The initial simulation domain was created using blockMeshDict, with even resolution in the x and y direction, and denser mesh resolution near the free surface in the vertical direction. The mesh was refined in the x-y direction using topoSetDict and refineMeshDict near the hull area. Six successive refinements were performed around the hull form to confirm the $y+$ criterion for proper viscous and pressure force capturing. For the drift simulations, the refinement areas were enlarged depending on the drift angle to accommodate the hull form. Next, snappyHexMeshDict was used to integrate the hull form into the simulation domain. The average mesh resolution used for the drift simulations was around 2.2 million, whereas the mesh resolution used for sway and yaw simulations was around 1.6 million. The minimum cell size in the x and y direction in the mesh is 0.0125m and z-direction is 0.01m. Further, four layers have been included around the hull form with a minimum layer thickness of 0.0025m.

In all the cases, the hull was rotated following the drift angle and then was integrated into the domain using snappyHexMesh. For the restricted water simulations, the mesh topology and cell size were kept the same. However, the refinements were extended both in the bottom and side section to better capture the interaction with the sides. The general mesh assembly used in the open and restricted water simulations is shown in Figure 2.

2.4. Computational resource.

All the simulations have been performed on a laptop with an intel core i7 processor and 8GB of RAM. The static drift simulations were run until 100s (simulation time) for steady results and each case took roughly 18 physical hours.

Table 1: Specifications of the bulk carrier ship model.

Specification	Symbol	Full scale	Model scale
Length between perpendicular	L _{pp} (m)	81.209	8.1209
Breadth	B (m)	14.0	1.4
Depth	D (m)	5.65	0.565
Draft	T (m)	4.35	0.435
Wetted surface area	S (m ²)	1668.44	16.68
Displacement volume	V (m ³)	4335500	4335.5

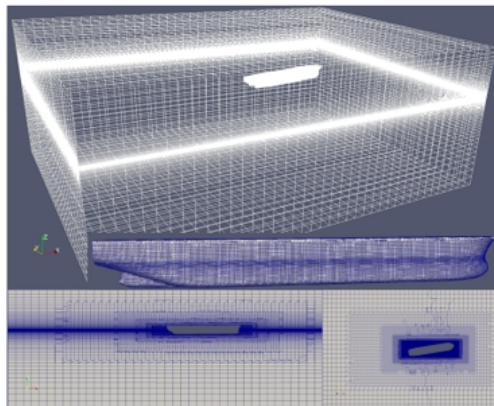
Source: Authors.

Figure 1: Side view of the 3000DWT inland bulk carrier vessel.

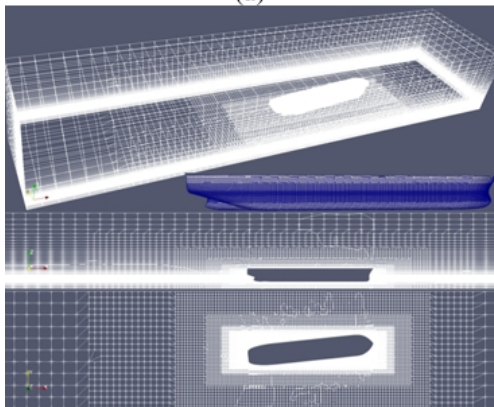


Source: Authors.

Figure 2: General mesh assembly used in the simulations: (a) the domain represents open water and (b) represents restricted channel (with limited depth and width).



(a)



(b)

Source: Authors.

3. Results.

Static drift simulation is the towing of a vessel in the oblique condition in a numerical towing tank. The vessel heading is adjusted based on the drift angle and then the vessel is towed forward. Since the vessel is in oblique condition, it experiences higher lateral force and yaw moment.

Static drift simulations have been performed for an inland bulk vessel with 3000 DWT in open and restricted waters. The open water simulations have been performed with a heave and pitch free motion. Whereas, for restricted waters, all motions have been kept restricted. All simulations have been performed at the design Froude number of 0.182 or model scale velocity of 1.627 m/s. Finally, using the simulation results, linear maneuvering derivatives have been calculated to assess the maneuvering capabilities of the vessel in both waterways.

3.1. Verification Study (open water simulations).

Initially, a verification study was performed to assess the uncertainty in the simulation results. Three different grid resolutions were used with a refinement ratio of 1.25, to perform the verification or uncertainty study following the ITTC 2011 guidelines. Both factor of safety and correction factor based approaches were used. The methods have been elaborately discussed by Islam and Guedes Soares, 2019. The uncertainty study was performed for the static drift case with 6 degrees drift angle. The mesh resolutions used are shown in Table 2. The cell size in the table indicates the minimum cell size in the x, y, and z-direction before the application of layers. Later, minimum cell size is shown after the application of layers.

Verification or uncertainty estimation has been performed for the surge and sway force, yaw moment, sinkage, and trim motion. Corrected uncertainty has been calculated using the

Table 2: Mesh resolutions used for the verification study for the PMM simulations.

Mesh No.	Total Mesh (million)	Cell size (X xY x Z)	Min. cell size (layer)	Grid Coarsening Ratio
Mesh 1 (Fine)	7.1	0.01 x 0.0099 x 0.0075	0.002	1
Mesh 2 (Mid)	4.03	0.0125 x 0.025 x 0.01	0.0025	1.25
Mesh 3 (Coarse)	1.8	0.0156 x 0.0156 x 0.015	0.00312	1.25

Source: Authors.

factor of safety and correction factor based approach. The summarized results are shown in Table 3.

The uncertainty estimation results show that all the results show convergence, except the sway force result, which is divergent. Nevertheless, the estimated uncertainty remains at a 5% level for all the cases following the correction factor based approach, and at around 1% for most cases following the factor of safety based approach. Thus, assuming a required level of uncertainty of 5%, the case can be considered validated.

Unfortunately, no model or full scale experimental study has been performed for the vessel before or after it was built. Thus, validation data for confirming the results are not available. Nevertheless, the low level of uncertainty in the results suggests that the estimations should be reliable.

3.2. Static Drift simulations in open waters.

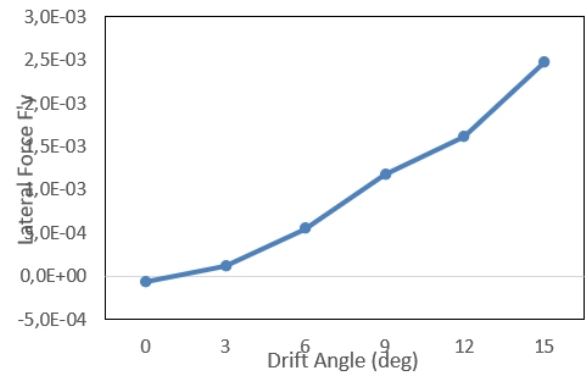
Six different drift angles have been studied from 0 to 12 degrees with a 3-degree interval. All simulations have been performed with a heave and pitch free motion to understand how vessel sinkage and trim change while maneuvering. From the simulations, surge force, sway force, yaw moment has been recorded, along with sinkage and trim. The results are shown in Table 4. For the non-dimensionalization of the results, the following equations have been used.

$$F'_Y = \frac{f_y \text{ (N)}}{\rho \times v^2 \times L_{pp}^2} \quad (4)$$

$$M'_Z = \frac{m_z \text{ (N)}}{\rho \times v^2 \times L_{pp}^3} \quad (5)$$

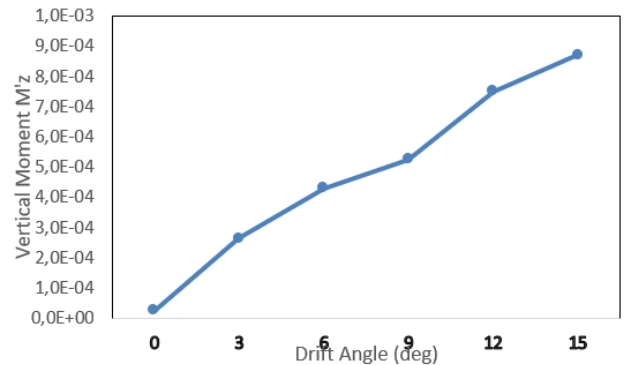
The lateral force and yaw moment variations based on drift angles are also shown in Figures 3 and 4, and the sinkage and trim history are shown in Figure 5. The force and moment show almost a linear correlation with the drift angle, and the experienced force and moment increase with increasing angle. As for motion results, the trim shows minor variation with drift angle. However, in full scale, the sinkage results would show a variation of 150 cm from 0 to 15-degree draft, which might be significant in the case of navigation through shallow channels.

Figure 3: Change in non-dimensional lateral force with changing drift angle in open water.



Source: Authors.

Figure 4: Change in non-dimensional yaw moment with changing drift angle in open water.



Source: Authors.

Table 3: Uncertainty estimation for the 6 deg static drift simulation results using ITTC 2011 guidelines.

Property		F _x (N)	F _y (N)	M _z (N-m)	Sinkage (mm)	Trim (deg)
Output values	Ø ₁ (fine)	-129.77	100	576.15	-12.13	-0.476
	Ø ₂ (mid)	-136.428	95.5	607.01	-12.585	-0.483
	Ø ₃ (coarse)	-132.96	94.04	601.08	-12.49	-0.496
Convergence	ε _{21/ε32}	-1.92	3.08	-5.20	-4.79	0.54
Grid convergence index (GCI)	GCI ²¹ _{fine}	0.0698	0.0271	0.0159	0.0124	0.0216
	GCI ³² _{fine}	0.0346	0.0092	0.0029	0.0025	0.0395
Factor of safety based approach						
Corrected uncertainty		1.40%	0.54%	0.32%	0.25%	0.43%
Correction factor based approach						
Corrected uncertainty		-5.13%	NA	5.36%	-3.75%	0.89%

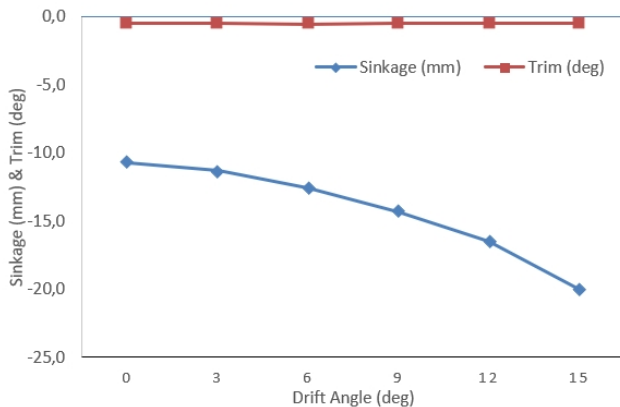
Source: Authors.

Table 4: Static drift simulation results for the 3000DWT inland bulk vessel.

Drift Angle	Drag force coef. C _t	Lateral force, F' _y	Yaw moment, M' _z	Sinkage (mm)	Trim (deg)
0	5.05E-03	-6.05E-05	2.46E-05	-10.720	-0.477
3	5.32E-03	1.21E-04	2.64E-04	-11.325	-0.480
6	6.19E-03	5.48E-04	4.29E-04	-12.585	-0.483
9	7.10E-03	1.18E-03	5.26E-04	-14.300	-0.475
12	8.22E-03	1.62E-03	7.51E-04	-16.490	-0.470

Source: Authors.

Figure 5: Change in sinkage and trim angle for the inland bulk carrier with changing drift angle.



Source: Authors.

3.3. Static Drift simulations in restricted waters.

For the restricted water simulations, a class III inland channel for Bangladesh has been considered. The class III routes are important for cargo transportation and thus were studied. Detail regarding the channel class and the simulation domain has been provided in section 2.3.

Static drift simulations have been performed for varying drift angles from 0 to 12 degrees with a 3-degree interval. The hull has been kept static for these cases with all motions restricted. This has been done since the force measurements were showing relatively high oscillation due to the shallow draft and

relatively high speed. However, the impact of heave and pitch free motion on force and moment measurements have been found to be minor for the initial case study. Thus, motions have been kept restricted for the simulations. As before, surge and sway force, and yaw moment have been recorded from the simulations, and equations 4 and 5 have been used for the non-dimensionalization of the results. The static drift simulation results for the restricted water are shown in Table 5.

Comparing to the simulation results for open water, all restricted water cases show notably higher forces and moment results. This added drag and moment is mostly caused by the shallow draft of the waterway and the interaction of the Kelvin wave with the side walls of the channel, as can be seen in Figure 8. Figure 8 shows pressure distribution on the free surface and the side of the hull for drift angles of 6, 9, and 12 degrees, for both open water (left) and restricted water (right) cases. All the images in the figure shows the same pressure range. The seemingly pitch like position of the hull in restricted channel cases is due to the drift angle and camera position. As expected, for both cases, the flow field shows gradually increasing pressure with increasing drift angle. However, for the shallow channel cases, the observed drag at the bottom of the hull is substantially higher. The free surface pressure distribution also shows a higher drag. Finally, a comparison among the time histories for the forces and moment for both the open and restricted water simulations is shown in Figure 9. A notable difference between the two sets of cases is the oscillation in forces and moment.

The restricted channel simulations show notable higher os-

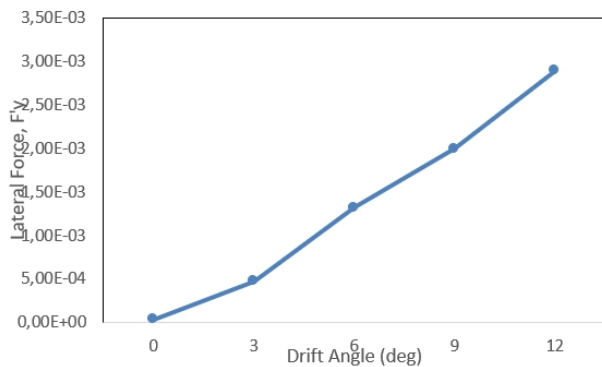
Table 5: Static drift simulation results for the 3000DWT inland bulk vessel in restricted water.

Drift Angle	Drag force coef. C_t	Lateral force, F'_y	Yaw moment, M'_z
0	1.21E-02	3.25E-05	1.13E-05
3	9.51E-03	4.72E-04	3.72E-04
6	1.02E-02	1.32E-03	5.97E-04
9	1.19E-02	1.99E-03	9.61E-04
12	1.48E-02	2.89E-03	1.34E-03

Source: Authors.

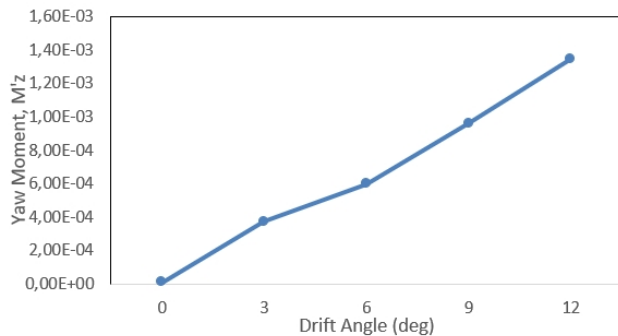
cillation in forces and moments, which is mostly attributed to the interaction with the channel bottom and sides. The restriction of heave and pitch motion also attributes to it.

Figure 6: Change in non-dimensional lateral force with changing drift angle in restricted water.



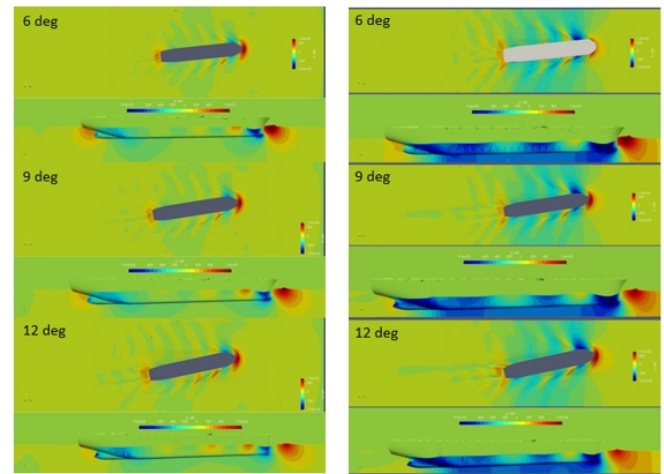
Source: Authors.

Figure 7: Change in non-dimensional yaw moment with changing drift angle in open water.



Source: Authors.

Figure 8: Hydrodynamic pressure distribution on the free surface and on the side of the hull for drift angles of 6, 9, and 12 degrees, for the open water (left) and restricted water (right) cases.



Source: Authors.

3.4. Derivatives calculation.

Hydrodynamic derivatives or coefficients represent the rate of change in force or moment, with the rate of change in direction and velocity or acceleration. The values of hydrodynamic derivatives help to determine the stability and maneuverability characteristics of a vessel. Generally, captive model tests (like Planar Motion Mechanism-PMM test) are used with conditions to derive added mass and damping coefficients (Lewis, 1988).

By using curve fitting to the data for forces and moments as a function of drift angle, the linear hydrodynamic derivatives or coefficients, Y_v and N_v can be predicted from the slopes. The predicted derivatives from the presented study are shown in Table 6.

Following theoretical hydrodynamics, Y_v is expected to be a relatively large value, whereas N_v is expected to be small. Thus, according to static derivatives, the vessel has relatively low lateral stability. The instability increases slightly with channel restrictions. The vessel shows relatively better yaw stability, which also decreases slightly in restricted conditions. However, overall, the vessel shows relatively good stability in both open and restricted channels, considering that it will only be operating in inland waters without waves.

Table 6: Hydrodynamic derivatives predicted from PMM simulations results for an inland bulk carrier.

Drift Angle	Drag force coef. C_t	Lateral force, F'_y	Yaw moment, M'_z
0	1.21E-02	3.25E-05	1.13E-05
3	9.51E-03	4.72E-04	3.72E-04
6	1.02E-02	1.32E-03	5.97E-04
9	1.19E-02	1.99E-03	9.61E-04
12	1.48E-02	2.89E-03	1.34E-03

Source: Authors.

Conclusions.

Static drift simulations have been performed to assess the maneuvering capabilities of an inland bulk carrier designed for the waterways of Bangladesh. After the initial verification study, static drift simulations have been performed in open water for varying drift angles. Next, drift simulations have been performed for the vessel in restricted waters with narrow width and shallow depth. Finally, linear derivatives have been calculated from the simulation results to assess the stability of the vessel while maneuvering.

The verification study showed that simulation uncertainty is limited to 5% for most of the results. Assuming a required uncertainty level of 5%, the study remains validated. Unfortunately, direct validation of simulation results was not possible for any of the cases due to the absence of experimental or sea trial data.

The static drift results for open water show an almost linear change in lateral force and yaw moment with changing drift angle. Although the change in trim angle remains very small due to changing drift angle, sinkage shows notable variation with changing drift angle. This is important information for vessels while passing through shallow channels.

The static drift simulations in restricted waters show a notable increase in experience forces and moment. The increase in forces and moment has been explained by the interaction of the vessel with the channel bottom and sides. The lateral force and yaw moment shows a linear trend with respect to changing drift angle, like in the case of open waters.

Finally, the linear hydrodynamic derivatives predicted from the simulation results show that the vessel has relatively good stability. Although channel restrictions increase the instability, the change remains minor. Nevertheless, this is only in the case of linear derivatives and the conclusion might change in the case of dynamic derivatives.

References.

Bangladesh Inland Water Transport Authority. [Online] Available at: <http://www.biwta.gov.bd> [Accessed: 2021].

Brogli, R., Muscari, R. and Mascio, A. D., 2008. Numerical simulations of the pure sway and pure yaw motion of the KVLCC1 and 2 tankers. SIMMAN 2008 Proceedings, , Papers, CFD Based Methods, p F2-9.

Cura-Hochbaum A, Vogt, M. and Gatchell, S., 2008. Manoeuvring prediction for two tankers based on RaNS simulations. SIMMAN 2008 Proceedings, Papers, CFD Based Methods, p F22-27.

Guilmineau E., Queutey P., Visonneau M., Leroyer A., and Deng, G., 2008. RANS simulation of a US NAVY frigate with PMM motions. SIMMAN 2008 Proceedings, Papers, CFD Based Methods, p F28-33

Hajivand A., Mousavizadegan S.H., 2015a. Virtual maneuvering test in CFD media in presence of free surface. International Journal of Naval Architecture and Ocean Engineering, 7:540–558.

Hajivand A., Mousavizadegan S.H., 2015b. Virtual simulation of maneuvering captive tests for a surface vessel. International Journal of Naval Architecture and Ocean Engineering, 7:848–872.

Islam H., Rahaman MM, Afroz L., Akimoto H., 2018. Estimation of linear hydrodynamic derivatives of a VLCC using static drift simulation. AIP Conference Proceedings 1980, 0400-21 (2018).

Islam H., Guedes Soares C., 2018a. Estimation of hydrodynamic derivatives of a container ship using PMM simulation in OpenFOAM. Ocean Engineering, 164:414-425.

Islam H., Guedes Soares C., 2018b. A CFD study of a ship moving with constant drift angle in calm water and waves. Progress in Maritime Engineering and Technology – Guedes Soares & Santos (Eds.) © 2018 Taylor & Francis Group, London, ISBN 978-1-138-58539-3.

Islam H., Guedes Soares C., 2019. Uncertainty analysis in ship resistance prediction using OpenFOAM, Ocean Engineering, 191:105805.

ITTC-2011. ITTC- Recommended Procedures and Guidelines: Practical Guidelines for Ship CFD Application. 7.5-03-02-03.

Jasak, H., 2009. OpenFOAM: Open Source CFD in research and industry. International Journal of Naval Architecture and Ocean Engineering, 1(2):89-94.

Kim H., Akimoto H., Islam H., 2015. Estimation of the hydrodynamic derivatives by RaNS simulation. Ocean Engineering, 108:129-139.

Lee, S. and Kim, B., 2015. A numerical study on manoeuvrability of wind turbine installation vessel using OpenFOAM. International Journal of Naval Architecture and Ocean Engineering, Volume 7, pp. 466-477.

Lewis, E., 1988. Principles of Naval Architecture. Jersey

City, NJ: The Society of Naval Architects and Marine Engineers.

Liu J., Hekkenberg R., Rotteveel E., Hopman H., 2015. Literature review on evaluation and prediction methods of inland vessel manoeuvrability. *Ocean Engineering*, 106:458-471.

Liu Jialun, 2017. Impacts of rudder configuration on inland vessel manoeuvrability. PhD Thesis, Delft University of Technology.

Miller, R. W., 2008. PMM calculation for the bare and appended DTMB 5415 using the RaNS solver CFDShip-IOWA. SIMMAN 2008 Proceedings, , Papers, CFD Based Methods, p F40-46.

Shen Z., Wan D. and Carrica Pablo M., 2015. Dynamic overset grids in OpenFOAM with application to KCS self-propulsion and maneuvering. *Ocean Engineering*, Volume 108, pp.

287-306.

SIMMAN 2008. [Online] Available at: <http://www.simman-2008.dk/> [Accessed 2016].

Simonsen Claus D., Otzen Janne F., Klimt C., Larsen Nikolaj L., 2012. Maneuvering predictions in the early design phase using CFD generated PMM data. 29th Symposium on Naval Hydrodynamics , Gothenburg.

Simonsen Claus D. and Stern F., 2008. RANS simulation of the flow around the KCS container ship in pure yaw. In: Proceedings of the SIMMAN 2008 workshop, , Papers, CFD Based Methods, p F55-62.

Yao, J., Jin, W. and Song, Y., 2016. RANS simulation of the flow around a tanker in forced motion. *Ocean Engineering*, Volume 127, pp. 236-245.